Proton Solubility in Undoped and Fe-doped $SrTiO_3$: Temperature Dependence and Formation of Defect Associates

Rainer Waser
Philips GmbH Forschungslaboratorium Aachen

Z. Naturforsch. **42a**, 1357–1365 (1987); received August 12, 1987

Dedicated to Professor Dr. Konrad Georg Weil on the Occasion of his 60th Birthday

The temperature dependence of the solubility of proton defects in $SrTiO_3$ single crystals was investigated by IR spectroscopy. Based on the integrated absorption of the OH stretching vibration bands, the enthalpies of the dissolution reaction were determined for undoped and Fe-doped $SrTiO_3$. In contrast to undoped $SrTiO_3$, which shows only one unique OH absorption frequency, characteristic sidebands were observed for Fe-doped crystals. These sidebands were attributed to the formation of associates between donor-type proton defects and Fe-acceptors in the perovskite lattice. From the temperature dependence of the sideband absorptions, an association enthalpy was estimated. The proton solubility and the sidebands were not affected by changing the oxygen partial pressure between approx. 10^{-15} and 10^5 Pa.

1. Introduction

Alkaline earth titanates of the perovskite structure type are of great technological importance for electronic ceramics used in passive components such as capacitors, non linear resistors, thermistors, etc. The high-temperature point defect chemistry and the defect equilibria, which are frozen-in at moderate temperatures, control the dielectric properties of components made from these materials. For this reason, their defect structure and defect-related properties were intensively studied in the last two decades (e.g., $BaTiO_3$ [1–4], $SrTiO_3$ [5–7], and $CaTiO_3$ [8, 9]).

Recently, these studies were supplemented by the author reporting on proton defects in barium and strontium titanates. The solubility [10] and the mobility [11] of proton defects were investigated as a function of the dopant concentration and the equilibrium water vapor pressure. The present paper focusses on the temperature dependence of the solubility and, in addition, reports on the formation of defect associates. The data were obtained using IR spectroscopy as a tool to measure the OH stretching vibration bands in undoped and Fe-doped $SrTiO_3$ single crystals. Using the same tool, the crystallographic aspects of protons in $SrTiO_3$ single crystals including the position and direction of the OH oscillator in the tetragonal, low-temperature phase and the cubic phase (above 105 K) were studied by Kapphan et al. [12, 13] in great detail. However, the defect structural aspects and the defect equilibria established during annealing of the crystals at high temperatures have not been considered.

To support the discussion (Sect. 5) of the experimental results, a brief review of the defect structure of alkaline earth titanates is given in the next section.

2. Defect structure

The defect structure of alkaline earth titanates $ATiO_3$ (A = Ca, Sr, Ba) was studied using techniques such as high-temperature electrical conductivity measurements and thermogravimetry [1–9]. It was found that, due to the close packed nature of the perovskite structure, vacancies are the dominant ionic defects. No evidence for metal or oxygen interstitials is reported. Undoped $ATiO_3$ is governed by a Schottky disorder which is established at very high temperatures ($T >$ approx. 1500 K) during the formation of the lattice. Due to their low mobilities, the generated metal vacancies are virtually frozen-in below temperatures of approx. 1500 K [14] and, thus, can be regarded as a fixed acceptor concentration. On the contrary, oxygen vacancies $V_o^{\cdot\cdot}$ are sufficiently mobile down to approx. 900 K to establish an equilibrium with the oxygen partial pressure P_{O_2} of the surrounding gas phase [15, 16]:

$$O_o \rightleftharpoons 1/2\, O_2 + V_o^{\cdot\cdot} + 2\,e'. \qquad (1)$$

Reprint requests to Dr. R.Waser, Philips GmbH Forschungslaboratorium Aachen, Weißhausstraße, D-5100 Aachen.

0932-0784 / 87 / 1100-1357 $ 01.30/0. – Please order a reprint rather than making your own copy.

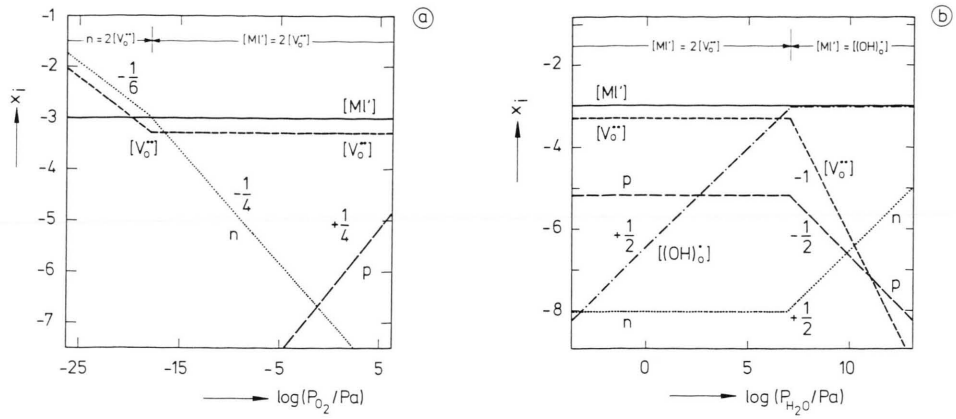

Fig. 1. Schematic illustration of the defect situation in acceptor-doped $SrTiO_3$ ($x_{Ml'} = 10^{-3}$) at approx. 1200 K. (a) Molar fractions x_i vs. P_{O_2}, assuming that the valence state of Ml′ does not change and $P_{H_2O} < 10^{-3}$ Pa. (b) Molar fractions x_i vs. P_{H_2O} at $P_{O_2} = 10^5$ Pa.

Acceptor dopants were found to be essential for the incorporation of protons from an H_2O atmosphere [10]. The acceptors can be either native metal vacancies or lower valent metal ions Ml substitutionally accommodated on A or Ti sites. For instance, Fe^{3+} replaces Ti^{4+} in $SrTiO_3$ forming a monovalent acceptor according to

$$Fe_2O_3 + 2\,BaO \rightarrow 2\,Ba_{Ba} + 2\,Fe'_{Ti} + V_o^{\cdot\cdot} + 5\,O_o. \quad (2)$$

In Fig. 1 a, the defect situation of an acceptor-doped $ATiO_3$ (molar fraction of the acceptor: $x_{Ml'} = 1 \cdot 10^{-3}$) as a function of P_{O_2} at a temperature of approx. 1175 K is schematically sketched. A dry atmosphere is assumed here, allowing proton defects to be neglected. Obviously, the majority disorder is dominated by the mutual compensation of acceptors Ml′ and oxygen vacancies $V_o^{\cdot\cdot}$ over a wide partial pressure range from oxidizing atmospheres down to very low P_{O_2} (approx. 10^{-18} Pa).

A thermal desorption technique was employed to study the solubility of protons in $BaTiO_3$ ceramics [10]. Based on the dependence of the solubility on the acceptor concentration and the water vapor pressure P_{H_2O}, the incorporation/desorption reaction

$$H_2O + V_o^{\cdot\cdot} + O_o \rightleftarrows 2(OH)_o^{\cdot} \quad (3)$$

was deduced. For each water molecule dissolved, one oxygen vacancy has vanished and two protons have formed. The protons are bound to oxygen ions on regular sites forming hydroxide ions. Instead of being termed hydroxide ions $(OH)_o^{\cdot}$, equivalently, the hydrogen defects can be regarded as interstitial protons $H^{\cdot}$. Both expressions will be used throughout the text, each where appropriate. The mass expression for (3) is

$$\frac{x^2_{(OH)_o^{\cdot}}}{P_{H_2O} \cdot x_{V_o^{\cdot\cdot}}} = K_H(T) = \exp(-\Delta G_H/RT), \quad (4)$$

where $K_H(T)$ denotes the mass action constant and ΔG_H is the Gibbs reaction enthalpy. The defect situation resulting from (3) and (4) is schematically sketched as a function of P_{H_2O} in Figure 1 b. Two regimes can be distinguished: At P_{H_2O} below approx. 10^7 Pa, the hydroxide ions are minority defects obeying Sieverts' square root law. At higher P_{H_2O}, a regime is expected with hydroxide ions as majority defects compensating the acceptors in replacement of the $V_o^{\cdot\cdot}$. In case of $BaTiO_3$, only the low P_{H_2O} regime was studied yet. For oxide showing different defect structures, as for example Y_2O_3, the hydroxide dominated regime was experimentally obtained and investigated [17, 18].

3. Experimental

The strontium titanate single crystals (Commercial Crystals Inc., Florida, USA) were prepared as described in [11]. Slabs of 2 mm thickness were used for this study. The crystals were annealed at defined conditions with respect to the temperature, the water vapor pressures P_{H_2O}, and oxygen partial pressures P_{O_2}. The temperature was varied in the range between

725 K and 1250 K. The time of the equilibration treatment and the quenching rate were adapted to the annealing temperature using the diffusion coefficients of protons [11]. The quenching was achieved by pushing the sample plate from the hot zone into the cold zone of the annealing furnace. As proved in a separate test, the quenching rate was greater than 30 K/s. At the highest temperature, 1250 K, this quenching rate guaranteed a sufficiently well freezing-in of the defect equilibrium, (3). At the lowest temperature, 725 K, an annealing time of 250 h ensured the constitution of the equilibrium.

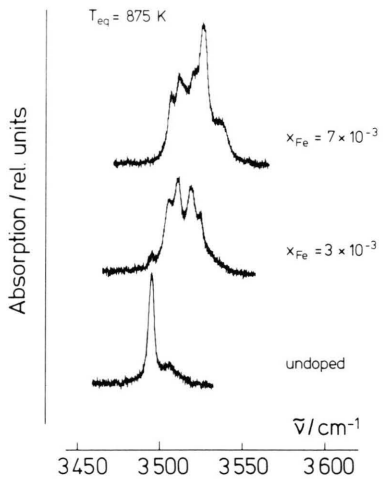

Fig. 2. OH stretching band absorption spectra at 296 K of undoped and differently Fe-doped $SrTiO_3$ annealed in $P_{H_2O} = 2.4 \cdot 10^3$ Pa and $P_{O_2} = 10^5$ Pa at 875 K.

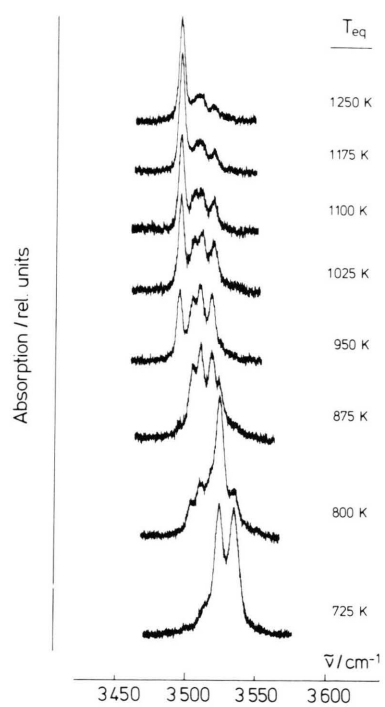

Fig. 3. OH stretching band absorption spectra at 296 K of Fe-doped $SrTiO_3$ ($x_{Fe} = 3 \cdot 10^{-3}$) annealed in $P_{H_2O} = 2.4 \cdot 10^3$ Pa and $P_{O_2} = 10^5$ Pa at various annealing temperatures T_{eq}.

After cooling, the transmission in the wavelength range from approx. 3450 to 3600 cm^{-1} was recorded at 296 K ($\pm$ 2 K) using the lowest scan mode (approx. 2 h/100 cm^{-1}) of a Pye Unicam SP 2000 spectrometer. To distinguish the measuring temperature from the annealing temperature, the latter is denoted T_{eq} in Figs. 2 and 3. Every reference to the temperature throughout this paper refers to the annealing temperature without explicitely noting the subscript.

4. Results

In Fig. 2, the absorption spectra of the OH stretching vibration are shown for undoped and differently Fe-doped $SrTiO_3$ single crystals which were annealed at 875 K in oxidizing atmosphere and $P_{H_2O} = 2.4 \cdot 10^3$ Pa. Undoped crystals of different suppliers have been tested throughout the investigation. As already observed by Kapphan et al. [13], the spectra of undoped crystals vary in the intensity of the sidebands on the higher-frequency side of the main OH absorption band at 3495 cm^{-1}. In the Fe-doped crystals annealed at 875 K, the sidebands (denoted with respect to the OH band at 3495 cm^{-1} of undoped $SrTiO_3$) are obviously dominant and may clearly be attributed to the dopant. In Fig. 3, the OH absorption spectra of Fe-doped $SrTiO_3$ are shown for a range of annealing temperatures.

A quantitative analysis of the OH spectra was based on Lambert-Beer's law

$$a_{OH}(\nu) = -\frac{1}{d} \ln \frac{I(\nu)}{I_0}, \tag{5}$$

where $I(\nu)$ denotes the transmittance as a function of the wavenumber and I_0 the background transmittance. For low transmittance values as obtained for the OH absorption in case of our crystals, (5) can be modified to

$$a_{OH}(\nu) = \frac{1}{d} \frac{\Delta I(\nu)}{I_0}. \tag{6}$$

Equation (6) holds with good approximation for $\Delta I(\nu) = I(\nu) - I_0 \ll I_0$. Following a procedure described by Johnson et al. [19], an integrated absorption A_{OH} representing the area below the absorption coefficient,

$$A_{OH} = \int a_{OH}(\nu)\,d\nu, \tag{7}$$

may be used as a value being proportional to the OH concentration. A_{OH} has the dimension cm^{-2}. The molar fraction of hydroxide ions can be estimated from

$$x_{OH} = (1.16 \cdot 10^{-6}\ cm^2)\ A_{OH}\,. \tag{8}$$

The estimation is based on the assumption of the same OH oscillator strength in $SrTiO_3$ as found for TiO_2 [19]. This assumption is justified within a first approximation because of the low interaction between the OH stretching vibration and the host lattice vibrations which is deduced from the small bandwidth of the OH absorption bands [20].

In Fig. 4, the integrated absorption A_{OH} is plotted on a logarithmic scale versus the reciprocal annealing temperature for undoped $SrTiO_3$. The same diagram is given in Fig. 5 for Fe-doped $SrTiO_3$. In addition, the A_{OH} values evaluated for the abrorption band at 3495 cm^{-1} are plotted in a separate curve (open symbols).

The dependence of A_{OH} on the water vapor pressure P_{H_2O} is shown in Fig. 6 for Fe-doped $SrTiO_3$ in oxidiz-

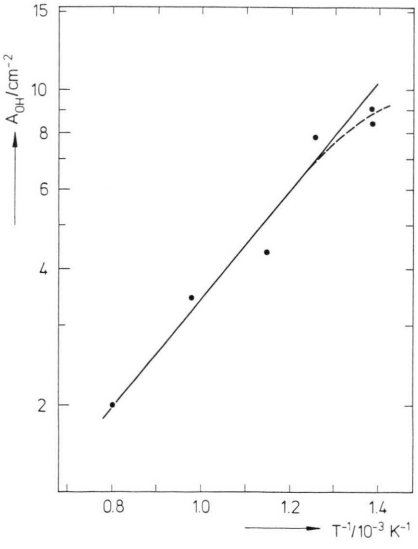

Fig. 4. Integrated absorption A_{OH} of undoped $SrTiO_3$ annealed in $P_{H_2O} = 2.4 \cdot 10^3$ Pa and $P_{O_2} = 10^5$ Pa vs. the reciprocal annealing temperature.

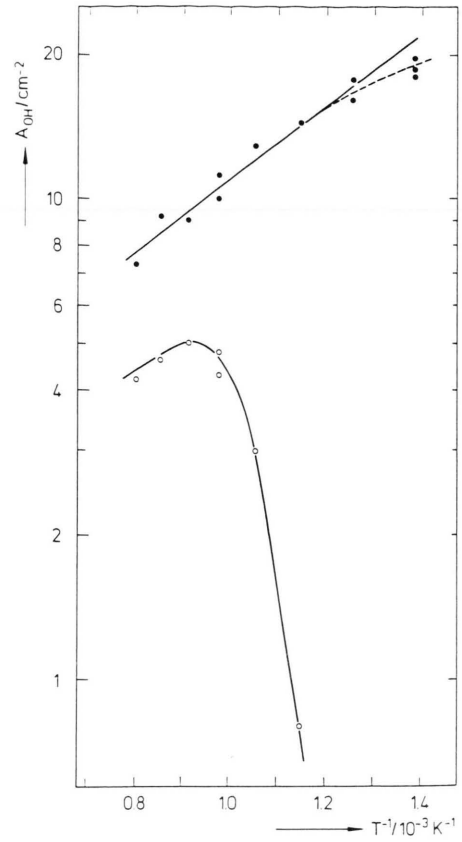

Fig. 5. Integrated absorption A_{OH} of Fe-doped $SrTiO_3$ ($x_{Fe} = 3 \cdot 10^{-3}$) annealed in $P_{H_2O} = 2.4 \cdot 10^3$ Pa and $P_{O_2} = 10^5$ Pa vs. the reciprocal annealing temperature. (●) A_{OH} of all OH lines, (○) A_{OH} of the OH line at 3495 cm^{-1}.

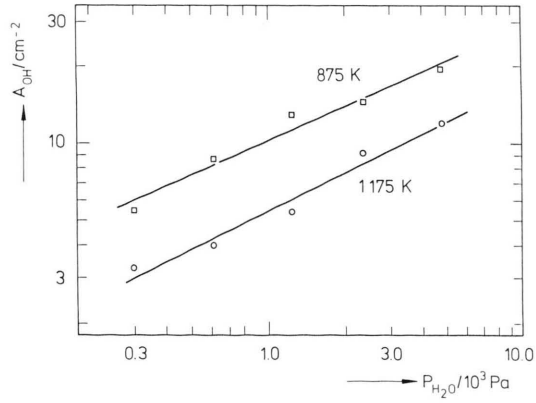

Fig. 6. Integrated absorption A_{OH} of Fe-doped $SrTiO_3$ ($x_{Fe} = 3 \cdot 10^{-3}$) vs. the equilibrium water vapor pressure P_{H_2O} after annealing at $T_{eq} = 875$ K and 1175 K and $P_{O_2} = 10^5$ Pa.

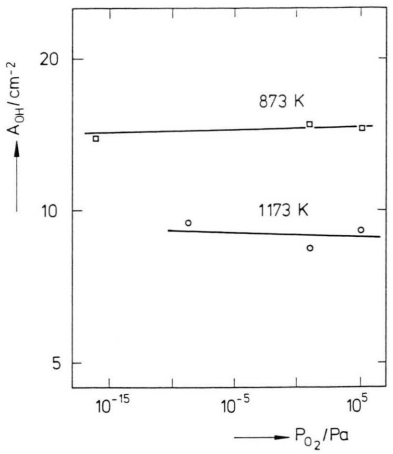

Fig. 7. Integrated absorption A_{OH} of Fe-doped $SrTiO_3$ ($x_{Fe} = 3 \cdot 10^{-3}$) vs. the oxygen partial pressure P_{O_2} after annealing at $T_{eq} = 875$ K and 1175 K and $P_{H_2O} = 2.4 \cdot 10^{-3}$ Pa.

ing atmospheres ($P_{O_2} = 10^5$ Pa). In an additional test, the oxygen partial pressure P_{O_2} was varied at fixed P_{H_2O}. The results are shown in Figure 7. The P_{O_2} at $1.6 \cdot 10^{-9}$ Pa and $6 \cdot 10^{-17}$ Pa have been established using moistened nitrogen with 10^2 Pa hydrogen. Because of $P_{H_2O} \gg P_{H_2}$, the actual water vapor pressure remains virtually unaffected.

5. Discussion

5.1. OH oscillators in undoped $SrTiO_3$

There are several crystallographic positions for the diatomic oscillator OH in the perovskite lattice of $SrTiO_3$ [12, 13]. Due to the cubic symmetry of the lattice above 105 K, these positions are energetically equivalent, which leads to one unique absorption line of the OH stretching vibration. In nominally pure $SrTiO_3$ at room temperature, this absorption line appears at 3495 cm^{-1} as shown at the bottom curve of Figure 2. Besides the main absorption line, weak sideband peaks are observed in some case as described in Section 4. Usually, the sideband lines are approx. 5 to 20 cm^{-1} apart from the main line on the higher energy side. The sideband peaks are assumed to be related to hydroxide ions, since they vanish with the main line after annealing the samples in dry atmospheres. Due to the fact that the intensity of the sidebands varies between samples from different supplies, they obviously must be attributed to impurities. Since no samples have been encountered yet which are absolutely free from sidebands, a possible intrinsic level of sidebands is open to question.

As will be described in the next section, the occurrence of the sidebands may be explained by the formation of defect associates between hydroxide ions and acceptors. The acceptors may be either native metal vacancies or impurities. Due to their natural abundances, impurities show acceptor character much more frequently than donor character [4]. For a given sample, the sideband intensities increase with decreasing equilibration temperature. This effect, as well, supports the idea of associate formation as discussed below.

5.2. Formation of defect associates

Association of point defects has been reported for several oxide systems. Often, the formation of associates of oxygen vacancies $V_o^{\cdot\cdot}$ and acceptor-type transition metal dopants is studied using the EPR technique. Detailed investigations into doped $SrTiO_3$ were performed in the last decades [21–25]. Using the same technique, the formation of associates of hydrogen defects (probably hydroxide ions) and Li'_{Mg} acceptors in Li-doped MgO was studied between liquid nitrogen temperature and room temperature. Thermodynamic data are not evaluated in these reports since absolute concentrations of defect associates are not readily obtainable by the EPR method.

In $SrTiO_3$, Ti sites are octahedrally surrounded by oxygen ions. If one of the oxygen ions becomes protonated, a hydroxide ion is formed and the absorption line at 3495 cm^{-1} is observed. In case of Fe-doped $SrTiO_3$, additional absorption lines appear on the high energy side of the spectrum as shown in Figure 2. The intensity of the sideband lines grows with increasing dopant concentration x_{Fe}. Furthermore, the intensity distribution shifts towards higher wavelength while the wavelengths of the sideband lines remain constant. All OH absorption lines observed in undoped and Fe-doped $SrTiO_3$ are listed in Table 1.

ν/cm^{-1}
3494.6
3504.3
3509.7
3518.6
3524.3
3536.4

Table 1. Wavenumbers ν of OH stretching vibrations observed in undoped and Fe-doped $SrTiO_3$ single crystals after annealing in $P_{H_2O} = 2.4 \cdot 10^3$ Pa and $P_{O_2} = 10^5$ Pa at various temperatures. The absorption line at 3494.6 cm^{-1} is the main line observed in undoped $SrTiO_3$. Reproducibility: ± 0.7 cm^{-1}.

The appearance of the sideband lines must obviously be attributed to the Fe-doping of $SrTiO_3$. Exchanging Ti^{4+} by Fe^{3+} will certainly influence the stretching vibration frequency of a neighbouring hydroxide ion. Due to the negative charge relative to the unperturbed $SrTiO_3$ lattice, Fe centers may attract the positively charged protons by Coulomb forces. The resulting defect associates {OH, Fe} are neutral with respect to the host lattice. Because of the cubic lattice symmetry, only one additional line would be expected for the occurrence of such an associate. However, a variety of similar associates is imaginable which may account for the different sideband lines found. For example, the hydroxide ion may not be on a nearest neighbour site to a Fe ion but on a next-nearest neighbour site. Or, the hydroxide ion may be attached to a $\{V_O, Fe\}$ associate which is expected to be present in high concentrations at low temperatures since Fe-acceptors and $V_O^{\cdot\cdot}$ are the majority defects in the system, and their association is supported by Coulomb interaction. Furthermore, a hydroxide ion may be situated between two adjacent Fe centers. Recently, an investigation has been started aiming at the crystallographic identification of the sideband lines [26].

Comparison of the main line and the sideband lines shows that the oscillator frequency and the linewidth are only slightly altered by the associate formation and, thus, may be regarded as a minor perturbation of the OH stretching vibration. Therefore, the relationship between the concentration of the species and their integrated absorption A_{OH} is assumed to be the same as described for the main absorption line in undoped $SrTiO_3$ in Section 4. By evaluating the absolute concentration of all different associates assigned to the sideband lines it would be possible to evaluate the individual mass action constants of their formation. However, as long as the diverse associates are not identified, this evaluation is not regarded to be reasonable. Instead, associated hydroxide ions and non-associated hydroxide ions will be distinguished using the degree of association

$$\chi = x_{OH}^{ass} / (x_{OH}^{free} + x_{OH}^{ass}) \tag{9}$$

as a measure of the relative concentration of the sum of all associates. In (9), x_{OH}^{free} and x_{OH}^{ass} denote the molar fractions of non-associated and associated hydroxide, respectively.

As shown for $x_{Fe} = 3 \cdot 10^{-3}$ doped $SrTiO_3$ in Fig. 3, the degree of association χ evidently increases with decreasing equilibration temperature. In addition, the intensity distribution of the absorption shifts towards lines of higher wavenumbers. A quantitative evaluation of the temperature evolution of the associate formation is presented in the next section.

An investigation similar to that shown for Fe-doped $SrTiO_3$ in Fig. 3 was performed for Ni-doped crystals ($x_{Ni} = 3 \cdot 10^{-3}$). Since the data are not yet completely evaluated, the results will be published elsewhere in detail [26]. However, anticipating this comprehensive evaluation, it can be stated qualitatively that Ni-doped $SrTiO_3$ shows an even more pronounced formation of associates than Fe-doped $SrTiO_3$ at a given temperature. This behaviour may be explained by the valency of the Ni-ions. As Fe-ions, Ni-ions are substitutionally incorporated on Ti sites. After equilibration in oxidizing atmospheres ($P_{O_2} = 10^5$ Pa), the majority of Ni-ions has a valency of +2 representing a divalent acceptor $Ni_{Ti}^{''}$. Thus, Ni-ions are much stronger Coulomb attractors for protons than Fe-ions which dominantly show a valency of +3 under the same equilibration conditions and therefore act as monovalent acceptors $Fe_{Ti}^{'}$ [27].

Mn-doped $SrTiO_3$ ($x_{Mn} = 1 \cdot 10^{-3}$) shows a completely different behaviour. The spectra are very similar to those of undoped $SrTiO_3$. They do not exhibit additional sideband lines, except those weak lines which are as well found for undoped $SrTiO_3$ with varying intensities and which may be due to associate formation of hydroxide ions with acceptor-type impurities or native metal vacancies (see Section 5.1). Furthermore, the total proton solubility in Mn-doped $SrTiO_3$ turned out to be very similar to undoped $SrTiO_3$. These findings may be attributed to the fact that Mn is incorporated on Ti sites with a valency of +4 [24] and, thus, represents an isovalent dopant. Consequently, Mn ions do not act as Coulomb attractors for protons and no driving force for associate formation exists.

5.3. Temperature dependence

The empirical temperature dependence of the proton solubility of undoped $SrTiO_3$ is shown in Figure 4. To evaluate this dependence, (4) may be rearranged to give the van't-Hoff-equation

$$\frac{d \ln K_H}{d (1/T)} = - \frac{\Delta H_H}{R}, \tag{10}$$

where ΔH_H denotes the enthalpy of dissolution.

P_{H_2O} was kept constant during the experimental series shown in Figure 4. Furthermore, hydroxide ions are minority species $x_{OH^\cdot} \ll x_{V_O^{\cdot\cdot}}$ and, as described in Sect. 2, the molar fraction $x_{V_O^{\cdot\cdot}}$ is fixed by the acceptor concentration which, in turn, is independent of the temperature. Thus, from the mass action (4)

$$\mathrm{d} \ln K_H = 2 \, \mathrm{d} \ln x_{OH} \tag{11}$$

can be derived. Using (8), (10), and (11), $\Delta H_H = -46.3 \pm 4.0$ kJ/mol was calculated from the linear regression curve shown in Figure 4 as a continuous line. The data at the lowest temperature of the series ($1/T = 1.38 \cdot 10^{-3}$ K^{-1}) were not included in the evaluation since they show a significant deviation from the straight line indicated as dashed curve in Figure 4. The reason for this deviation is not yet known. At first glance, it could be caused by an incompletely settled equilibrium due to too long diffusion times. However, experiments with different annealing times render this interpretation less probable.

The temperature dependence of the total proton solubility in Fe-doped $SrTiO_3$ was evaluated in a similar way from the data (solid circles) of Figure 5. ΔH_H calculates to -29.3 ± 2.1 kJ/mol. As in case of the undoped crystals, a significant deviation from the van't-Hoff behaviour occurs at the low temperature end of the series.

The results show that the proton solubility in undoped as well as in Fe-doped $SrTiO_3$ is significantly temperature dependent. This must be related to the fact that protons are minority defects (see Sect. 2 and 5.4). If protons are majority defects compensating a fixed acceptor concentration as, for example, reported for Y_2O_3 [18], the proton solubility is almost independent of the temperature.

The formation of defect associates is a typical example of an homogeneous solid state reaction [28]. Due to the Coulomb interaction as the driving force, the reaction is exothermic in nature and consequently the association decreases with rising temperature. As indicated in Sect. 5.2, the individual associates, which are assumed to have formed, will not be treated separately. Instead, an overall association/dissociation reaction

$$OH_O^\cdot + Ml' \rightleftharpoons \{OH, Ml\} \tag{12}$$

will be considered, where the right term formally comprises all types of associates. The mass action equation of this reaction may be expressed as a function of the degree of association χ introduced by (9)

$$\frac{\chi}{(1-\chi)\, x_{Ml'}} = K_A(T) = \exp\left(-\Delta G_A / RT\right). \tag{13}$$

$x_{Ml'}$ denotes the molar fraction of non-associated acceptors which is approximately the same as the total molar fraction of acceptors because hydroxide ions are minority species: $x_{Ml'} \gg x_{OH^\cdot} + x_{\{OH,\, Ml\}}$. To evaluate the formal mass constant $K_A(T)$, the A_{OH} data of the main absorption line at 3 495 cm^{-1} were calculated from Fig. 3 and are included in Fig. 5 as open circles. At a temperature of 950 K ($1/T = 1.05 \cdot 10^{-3}$ K^{-1}) for example, χ is approx. 0.75 and K_A calculates to $1.0 \cdot 10^3$ using the molar fraction of Fe-acceptors. From the slope at $1/T = 1.05 \cdot 10^{-3}$ K^{-1} in Fig. 5, an association enthalpy ΔH_A of approx. 150 kJ/mol can be calculated using the van't-Hoff-equation. It should be kept in mind, however, that ΔH_A is purely a formal value since in reality there is not only one equilibrium (12) but a superposition of several associate formation reactions.

It is important to note that the IR spectra quenched from annealing temperatures above 1 025 K exhibit more or less the same shape (Fig. 3) and the same degree of association. If this were a real feature it could only be explained by a very strong temperature dependence of ΔH_A. It is more likely, however, that this effect is caused by an insufficient quenching rate. To establish the equilibrium, the quenching always compedes with the diffusion coefficient and the mean diffusion length of the species to freeze. The freezing of the total proton dissolution reaction (3) is determined by a diffusion length in the order of the crystal thickness. The quenching rate is sufficient to conserve this equilibrium. The associate formation (12), however, is governed by a diffusion length of microscopic extension within the lattice. The quenching rate probably is too small to ensure the freezing of this equilibrium. Consequently, the actual equilibrium of the association corresponds to a lower temperature as intended.

5.4. Water vapor pressure dependence

The proton solubility in Fe-doped $SrTiO_3$, which can be evaluated from the integrated absorption by (8), was determined as a function of the water vapor pressure P_{H_2O} for two annealing temperatures. From the logarithmic diagram, Fig. 6, the slopes 0.45 and 0.49 are evaluated for $T = 875$ K and 1 175 K, respectively. Within good approximation, these slopes ap-

proach the square root law of Sieverts' schematically shown for the hydroxide concentration in Figure 1 b. This result is a further confirmation of the dissociation of water molecules in $SrTiO_3$, (3), in the same way as it was found for deuterons in acceptor-doped $BaTiO_3$ ceramics by a thermal desorption method [10].

There are indications that the degree of association increases with rising P_{H_2O} at a given annealing temperature. Details will be reported in a future paper.

5.5. *Oxygen partial pressure dependence*

For a further elucidation of the defect structure, the oxygen partial pressure dependence of the proton solubility is of considerable importance. As shown in Fig. 7, the P_{O_2} was varied over a large range at constant P_{H_2O} for two different annealing temperatures. The proton solubility, expressed as A_{OH}, remains constant within the reproducibility limits of the IR method. In addition, the shape of the spectra and, thus, the associate formation are not affected by the P_{O_2}. Comparing Fig. 1 a, the investigated range of P_{O_2} is in the regime of mutual compensation of acceptors and oxygen vacancies. Obviously, in this regime, the solubility and association of protons, as minority defects, are not affected by the oxygen partial pressure. This implies that the defect structure of proton dissolution in $SrTiO_3$ is completely described by the equations stated in Sect. 2 and no further reaction has to be considered. No statement, however, can be made yet about the behaviour of hydrogen defects in strongly reducing atmospheres, i.e. the P_{O_2} regime determined by electrons and oxygen vacancies (Figure 1 a).

Optical studies have shown that a small portion of the Fe-doping in $SrTiO_3$ is in the $+4$ valency state after equilibration in oxidizing atmosphere ($P_{O_2} = 10^5$ Pa) [27]. Fe^{4+} acts as isovalent dopant. Therefore, it is supposed that Fe^{4+} shows little tendency to stimulate associate formation similar to Mn^{4+} mentioned above. On the other hand, the portion of Fe^{3+} is only slightly affected so that a possible change in A_{OH} (Fig. 7) is below the reproducibility limit.

6. Conclusion

In the temperature range and water vapor pressure range covered by this investigation protons are minority defects in $SrTiO_3$. The incorporation reaction of water molecules from the gas phase to form proton defects is found to be exothermic. Enthalpy values of -46.3 ± 4.0 kJ/mol for undoped $SrTiO_3$ and -29.3 ± 2.1 kJ/mol for Fe-doped $SrTiO_3$ ($x_{Fe} = 3 \cdot 10^{-3}$) are determined. Besides the absorption line of the OH stretching vibration at 3 495 cm^{-1} observed in undoped $SrTiO_3$ single crystals, characteristic sideband lines are found in Fe-doped $SrTiO_3$. The sideband lines and their intensity depend on the dopant concentration and the annealing temperature. A suggestion is made attributing these lines to defect associates between hydroxide ions and acceptors. From the temperature dependence, a formal association enthalpy of approx. -150 kJ/mol is evaluated.

A study of the oxygen partial pressure dependence of the OH absorption reveals that the proton solubility as well as the associate formation is not affected by a variation of P_{O_2} in the wide range between 10^5 Pa and approx. 10^{-16} Pa (at 875 K). Thus, the defect structure of $SrTiO_3$ as far as related to the interaction with O_2 and H_2O can be regarded as completely determined by the individual incorporation reactions, (1) and (3). No further cross reactions have to be considered.

[1] H. Veith, Z. angew. Phys. **20,** 16 (1965).
[2] N.-H. Chan and D. M. Smyth, J. Electrochem. Soc., **123,** 1584 (1976).
[3] J. Daniels, K. H. Härdtl, D. Hennings, and R. Wernicke, Philips Res. Rept. **31,** [6] 487–566 (1976).
[4] D. M. Smyth, in: "Microstructure and Properties of Ceramic Materials", T. S. Yen and J. A. Pask (Eds.), Proceedings of the First China-US Seminar, p. 399, North-Holland Publishing, Amsterdam 1984
[5] H. P. R. Frederikse, W. R. Thurber, and W. R. Hosler, Phys. Rev. A **134,** 442 (1964).
[6] L. C. Walter and R. E. Grace, J. Phys. Chem. Solids **28,** 239 (1967).
[7] N. G. Eror and U. Balachandran, J. Solid State Chem. **42,** 227 (1982).
[8] U. Balachandran, B. Odekirk, and N. G. Eror, J. Mater. Sci. **17,** 1656 (1982).
[9] N. G. Eror and U. Balachandran, J. Solid State Chem. **43,** 196 (1982).
[10] R. Waser, submitted to J. Amer. Ceram. Soc.
[11] R. Waser, Ber. Bunsenges. Phys. Chem. **90,** 1223 (1986).
[12] S. Kapphan, J. Koppitz, and G. Weber, Ferroelectrics **25,** 585 (1980).
[13] G. Weber, S. Kapphan, and M. Wöhlecke, submitted to Phys. Rev. B.
[14] R. Wernicke, phys. stat. sol. (a) **47,** 139 (1978).

[15] A. E. Paladino, J. Amer. Ceram. Soc. **48,** 476 (1965).
[16] R. Wernicke, PhD-Thesis, Rheinisch-Westfälische Technische Hochschule Aachen, 1975.
[17] T. Norby and P. Kofstad, J. Amer. Ceram. Soc. **67,** 786 (1984).
[18] T. Norby and P. Kofstad, J. Amer. Ceram. Soc. **69,** 780 (1986).
[19] O. W. Johnson, J. DeFord, and J. W. Shaner, J. Appl. Phys. **44,** 3008 (1973).
[20] S. Kapphan and M. Wöhlecke, private communication.
[21] E. S. Kirkpatrick, K. A. Müller, and R. S. Rubins, Phys. Rev. **135,** A86 (1964).
[22] H. D. Meierling, phys. stat. sol. (b) **43,** 191 (1971).
[23] P. Koidl, K. W. Blazey, W. Berlinger, and K. A. Müller, Phys. Rev. B **14,** 2703 (1976).
[24] R. A. Serway, W. Berlinger, K. A. Müller, and R. W. Collins, Phys. Rev. B **16,** 4761 (1977).
[25] R. Berney, D. Cowan, and F. Morin, solid state comm. **26,** 579 (1978).
[26] S. Kapphan, R. Waser, and M. Wöhlecke, to be published.
[27] H.-J. Hagemann, PhD-Thesis, Rheinisch-Westfälische Technische Hochschule Aachen, 1980.
[28] H. Schmalzried and A. Navrotsky, Festkörperthermodynamik, Verlag Chemie, Weinheim 1975.